Thermodynamic Properties of Aqueous $(NH_4)_2SO_4$ to High Supersaturation as a Function of Temperature

Simon L. Clegg,*,† Sau Sau Ho,‡ Chak K. Chan,*,‡ and Peter Brimblecombe†

School of Environmental Sciences, University of East Anglia, Norwich NR4 7TJ, U.K., and Department of Chemical Engineering, Hong Kong University of Science and Technology, Clear Water Bay, Kowloon, Hong Kong

Equilibrium water vapor pressures over supersaturated aqueous ammonium sulfate have been determined from 278.15 to 313.15 K using an electrodynamic balance. Partial molar enthalpies of water (L_1, to ~25 mol kg^{-1}) and partial molar heat capacities (J_1, to ~8 mol kg^{-1}) have been calculated from the measurements, together with enthalpies of solution, heat capacities, and boiling point elevations. The results have been used to parameterize a mole-fraction-based activity coefficient model. Equilibrium constants for the reaction $(NH_4)_2SO_{4(cr)} \rightleftarrows 2NH_4^+{}_{(aq)} + SO_4^{2-}{}_{(aq)}$ have been evaluated from 373.15 K to the eutectic point (5.00 mol kg^{-1}, 254.21 K). The model satisfactorily represents water vapor pressures and saturation with respect to solid phases ice and ammonium sulfate from 253 to >373.15 K and up to 8–10 mol kg^{-1}, and water vapor pressures from 278.15 to 313.15 K and up to ~25 mol kg^{-1}.

1. Introduction

Ammonium sulfate is an important component of aqueous atmospheric aerosols in both remote and urban regions (*1*, *2*). Experiments on single, suspended particles (*3*, *4*) show that, at low relative humidity, aerosols can readily supersaturate with respect to dissolved salts such as ammonium sulfate and sodium chloride before crystallization occurs. Calculations of the behavior of aqueous atmospheric aerosols therefore require a knowledge of the properties of supersaturated solutions, including mixtures, over a range of temperatures. Ideally, this should be integrated within a self-consistent thermodynamic model in order to predict the properties of multicomponent solutions for different compositions and temperatures.

In previous work we have parameterized the mole-fraction-based thermodynamic (activity coefficient) model of Pitzer, Simonson, and Clegg (*5*) for the systems H_2SO_4–H_2O from <200 to 328 K (*6*), and $(NH_4)_2SO_4$–H_2SO_4–H_2O at 298.15 K (*7*). Here we present new measurements, using an electrodynamic balance, of water activities of supersaturated aqueous $(NH_4)_2SO_4$ from 278.15 to 313.15 K. The results are combined with literature data for activities, thermal properties, and aqueous solubilities to yield functions enabling the calculation of osmotic and activity coefficients of aqueous $(NH_4)_2SO_4$ from 0 to ~25 mol kg^{-1} and from <273.15 to about 373 K. The results are also used to extend the parameterization of the activity coefficient model for the $(NH_4)_2SO_4$–H_2O component (*7*), which is an important step in the generalization of the model for aqueous mixtures including dissolved $(NH_4)_2SO_4$.

2. Theory

The purpose of the present work is to obtain a self-consistent description of the thermodynamic properties of aqueous $(NH_4)_2SO_4$, and to apply the mole-fraction-based model of Pitzer, Simonson, and Clegg to the results. This is necessary in order to extend the model description of multicomponent systems containing $(NH_4)_2SO_4$ from a single temperature (e.g., 298.15 K in the case of $(NH_4)_2SO_4$–H_2SO_4–H_2O (*7*)) to a range of temperatures. The model equations and fundamental thermodynamic relationships are now given.

The solvent and all species concentrations and activity coefficients are expressed on a mole fraction basis. The mole fraction x_i of species i is given by

$$x_i = n_i/(\sum_j n_j) \tag{1}$$

where n_i is the number of moles of component i and the summation j is over all solution components including the solvent. The activities a_i of all components i are given by $a_i = f_i x_i$ where f_i is the activity coefficient. The reference state for the activity coefficients of solute species is one of infinite dilution with respect to the solvent, 1. Activity coefficients on this basis (rather than the pure liquid reference state) are denoted f_i^*; thus, $f_i^* \rightarrow 1$ as $x_1 \rightarrow 1$. The reference state for the activity coefficient of the solvent is the pure liquid, so that $f_1 \rightarrow 1$ as $x_1 \rightarrow 1$. The mole fraction scale activity coefficients given above are, for solute species, related to the more commonly encountered molality-based coefficients γ_i by (*8*)

$$f_i^* = \gamma_i(1 + M_1\sum_j m_j) \tag{2}$$

where M_1 (kg mol^{-1}) is the molar mass of the solvent and m_j (mol kg^{-1} of solvent) is the molality of solute species j. The activity coefficient of the solvent, f_1, is related to the rational (mole fraction) osmotic coefficient g and molal osmotic coefficient ϕ by

$$\ln(a_1) = g\ln(x_1) = \ln(x_1) + \ln(f_1) \tag{3a}$$

$$\ln(a_1) = -M_1\phi\sum_j m_j \tag{3b}$$

where the summation in eq 3b (as in eq 2) is over all solute species (here only NH_4^+ and SO_4^{2-}).

* To whom correspondence should be addressed.
† University of East Anglia.
‡ Hong Kong University of Science and Technology.

0021-9568/95/1740-1079$09.00/0

$$\ln(a_1) = \ln(x_1) + 2A_x I_x^{3/2}/(1 + \varrho I_x^{1/2}) - x_M x_X B_{MX} \exp(-\alpha_{MX} I_x^{1/2}) - x_M x_X B^1_{MX} \exp(-\alpha^1_{MX} I_x^{1/2}) + x_I^2(W_{1,MX} + (x_I - x_1)U_{1,MX}) + 4x_1 x_M x_X(2 - 3x_1)V_{1,MX} \quad (4)$$

$$\ln(f_M^*) = -z_M^2 A_x[(2/\varrho)\ln(1 + \varrho I_x^{1/2}) + I_x^{1/2}(1 - 2I_x/z_M^2)/(1 + \varrho I_x^{1/2})] + x_X B_{MX} g(\alpha_{MX} I_x^{1/2}) - x_M x_X B_{MX}[z_M^2 g(\alpha_{MX} I_x^{1/2})/(2I_x) + (1 - z_M^2/(2I_x))\exp(-\alpha_{MX} I_x^{1/2})] + x_X B^1_{MX} g(\alpha^1_{MX} I_x^{1/2}) - x_M x_X B^1_{MX}[z_M^2 g(\alpha^1_{MX} I_x^{1/2})/(2I_x) + (1 - z_M^2/(2I_x))\exp(-\alpha^1_{MX} I_x^{1/2})] + x_1((z_M + z_X)/(2z_X) - x_I)W_{1,MX} + x_1 x_I((z_M + z_X)/z_X - 2x_I)U_{1,MX} + 4x_1^2 x_X(1 - 3x_M)V_{1,MX} - (1/2)[(z_M + z_X)/z_X]W_{1,MX} \quad (5)$$

$$\ln(f_X^*) = -z_X^2 A_x[(2/\varrho)\ln(1 + \varrho I_x^{1/2}) + I_x^{1/2}(1 - 2I_x/z_X^2)/(1 + \varrho I_x^{1/2})] + x_M B_{MX} g(\alpha_{MX} I_x^{1/2}) - x_M x_X B_{MX}[z_X^2 g(\alpha_{MX} I_x^{1/2})/(2I_x) + (1 - z_X^2/(2I_x))\exp(-\alpha_{MX} I_x^{1/2})] + x_M B^1_{MX} g(\alpha^1_{MX} I_x^{1/2}) - x_M x_X B^1_{MX}[z_X^2 g(\alpha^1_{MX} I_x^{1/2})/(2I_x) + (1 - z_X^2/(2I_x))\exp(-\alpha^1_{MX} I_x^{1/2})] + x_1((z_M + z_X)/(2z_M) - x_I)W_{1,MX} + x_1 x_I((z_M + z_X)/z_M - 2x_I)U_{1,MX} + 4x_1^2 x_M(1 - 3x_X)V_{1,MX} - (1/2)[(z_M + z_X)/z_M]W_{1,MX} \quad (6)$$

$${}^\phi L = \nu z_M z_X(A_{Hx}/2\varrho)\ln(1 + \varrho I_x^{1/2}) - \nu x_I(z_M z_X/(z_M + z_X)^2)RT^2 B^L_{MX} g(\alpha_{MX} I_x^{1/2}) - \nu x_1(z_M z_X/(z_M + z_X)^2)RT^2 B^{1,L}_{MX} g(\alpha^1_{MX} I_x^{1/2}) + \nu RT^2 x_I(W^L_{1,MX} - x_1 U^L_{1,MX} - 4x_1^2(z_M z_X/(z_M + z_X)^2)V^L_{1,MX}) \quad (7)$$

$${}^\phi C_p = {}^\phi C_p^\circ + \nu z_M z_X(A_{Cx}/2\varrho)\ln(1 + \varrho I_x^{1/2}) - \nu x_I(z_M z_X/(z_M + z_X)^2)RT^2 B^J_{MX} g(\alpha_{MX} I_x^{1/2}) - \nu x_1(z_M z_X/(z_M + z_X)^2)RT^2 B^{1,J}_{MX} g(\alpha^1_{MX} I_x^{1/2}) + \nu RT^2 x_I(W^J_{1,MX} - x_1 U^J_{1,MX} - 4x_1^2(z_M z_X/(z_M + z_X)^2)V^J_{1,MX}) \quad (8)$$

The model equations for water activity (a_1) and the mole fraction activity coefficient of cation M (f_M^*) and anion X (f_X^*) in a pure aqueous solution of salt $M_{\nu+}X_{\nu-}$ are given in eqs 4–6.

In the equations, A_x is the Debye–Hückel parameter on a mole fraction basis (2.917 at 298.15 K), I_x ($=0.5\sum_i x_i z_i^2$) is the mole fraction ionic strength, and ϱ is a constant set equal to 13.0. The charge magnitudes of ions M and X are z_M and z_X, respectively. Terms including the parameter B_{MX} (and B^1_{MX}), associated coefficients α_{MX} (and α^1_{MX}), and function $g(x)$ comprise an extended Debye–Hückel function. Further terms in x_1 and x_I (the total mole fraction of ions, here $x(NH_4^+) + x(SO_4^{2-})$), involving parameters $W_{1,MX}$, $U_{1,MX}$, and $V_{1,MX}$, describe the short-range interactions that dominate in concentrated solutions. The values of the model parameters are determined by fitting to empirical data (*5*, *7*).

The model equations for the apparent molar enthalpy ${}^\phi L$ (J mol^{-1}) and apparent molar heat capacity ${}^\phi C_p$ (J mol^{-1} K^{-1}) are given in eqs 7 and 8. In the equations ν is the number of moles of ions produced by the dissociation of one mole of salt ($\nu_- + \nu_-$ for $M_{\nu+}X_{\nu-}$), A_{Hx} is the Debye–Hückel enthalpy parameter, equal to $4RT^2(\partial A_x/\partial T)_P$, R (8.3144 J mol^{-1} K^{-1}) is the gas constant, and T (K) is temperature. For each model parameter P with superscript L (B^L_{MX}, $B^{1,L}_{MX}$, $W^L_{1,MX}$, $U^L_{1,MX}$, and $V^L_{1,MX}$) in eq 7

$$P^L = \partial P/\partial T \quad (9)$$

with pressure held constant. Similarly, for parameters with superscript J in eq 8

$$P^J = \partial^2 P/\partial T^2 + (2/T)\,\partial P/\partial T \quad (10)$$

Both ϱ and all α are treated as being invariant with temperature. In eq 8 ${}^\phi C_p^\circ$ is the infinite dilution value of the apparent molar heat capacity at temperature T, and A_{Cx} is the Debye–Hückel heat capacity parameter (equal to $(\partial A_{Hx}/\partial T)_P$). All Debye–Hückel parameters used in this work were calculated using the equations presented in Appendix 1 of Clegg and Brimblecombe (*6*).

The apparent molar enthalpy (${}^\phi L$) is related to the enthalpy of dilution $\Delta_{dil}H(m_1 \rightarrow m_2)$ from molality m_1 to m_2 by $\Delta_{dil}H(m_1 \rightarrow m_2) = {}^\phi L_2 - {}^\phi L_1$. Also, the integral enthalpy of solution $\Delta_{sol}H$ for the dissolution of solid $(NH_4)_2SO_4$ is the heat effect for the reaction

$$(NH_4)_2SO_{4(cr)} + n_1 H_2O_{(l)} \rightarrow (NH_4)_2SO_4(aq, n_1 H_2O) \quad (11)$$

and is related to the apparent molar enthalpy by ${}^\phi L = \Delta_{sol}H - \Delta_{sol}H^\circ$, where $\Delta_{sol}H^\circ$ is the enthalpy of solution per mole of salt at infinite dilution.

The partial molar enthalpy L_1 (J mol^{-1}), equivalent to $-RT^2(\partial \ln(a_1)/\partial T)_{P,x}$, and heat capacity of the solvent J_1, equal to $\partial L_1/\partial T$, are also required here and are related to the solvent activity by

$$\ln(a_{1,T}) = \ln(a_{1,T_r}) + yL_1 - zJ_1 \quad (12a)$$

$$y = (T_r - T)/(RTT_r) \quad (12b)$$

$$z = T_r y - \ln(T_r/T)/R \quad (12c)$$

where T (K) is the temperature of interest and T_r a reference temperature (here 298.15 K). The above equation assumes that J_1 is invariant with temperature. Quantities L_1 and J_1 can be calculated from the corresponding apparent molar properties *via* standard equations (*9*)

$$L_1 = -(1/2)M_1 m^{3/2}\,\partial {}^\phi L/\partial m^{1/2} \quad (13)$$

$$J_1 = -(1/2)M_1 m^{3/2}\,\partial {}^\phi C_p/\partial m^{1/2} \quad (14)$$

where m denotes solute molality.

Finally we consider the equilibrium between aqueous ammonium sulfate and the solid salt:

$$(NH_4)_2SO_{4(cr)} \rightleftharpoons 2NH_4^+{}_{(aq)} + SO_4^{2-}{}_{(aq)} \quad (15)$$

The equilibrium constant K_s (mole fraction basis), which is a function of temperature, is given by

$$K_s = a(NH_4^+)^2 a(SO_4^{2-})/a((NH_4)_2SO_{4(cr)}) \quad (16)$$

where a denotes activity. The activity of the pure solid

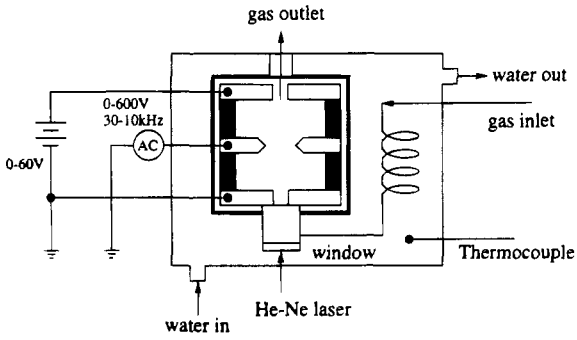

Figure 1. Schematic diagram of a temperature-controlled electrodynamic balance. The position of the particle (not shown) is maintained in the center of the balance. Note that the laser is oriented horizontally in the built apparatus, and not vertically as shown here for ease of presentation.

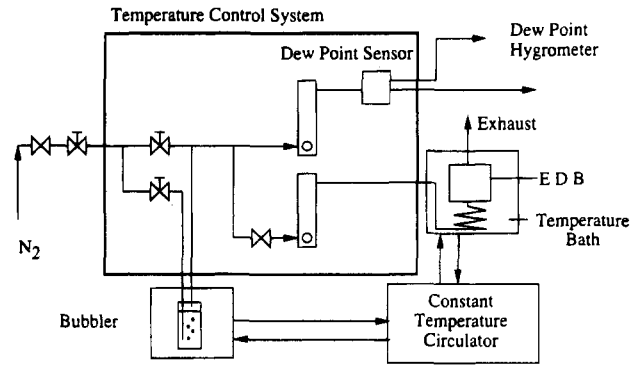

Figure 2. Control of temperature and relative humidity (RH) during water activity measurement. On the right of the figure "EDB" is the electrodynamic balance.

phase $a((NH_4)_2SO_{4(cr)})$ is by definition unity, leaving only the activity product of the ions in eq 16.

3. Experiments

The concentration dependence of the water activity of $(NH_4)_2SO_4$ solutions was determined from 278.15 to 313.15 K by single particle levitation, using an electrodynamic balance (EDB) to trap and hold a particle of approximately 20 μm diameter stationary in an electric field. This technique has a wide application in aerosol research (*10*), and is well suited to measuring water activities of aqueous droplets (*11*). Since a droplet can be freely levitated without contact with any foreign surfaces, heterogeneous nucleation can be suppressed, allowing the study of supersaturated solutions.

(a) Apparatus. The principles and applications of the EDB have been reviewed in detail by Davis and others (*10*, *12*). Briefly, in an EDB, a combination of ac and dc fields is used to trap and levitate a charged particle. Here, we used a three-ring EDB with insulation spacers between the electrodes, similar to the apparatus used previously by Chan *et al.* (*13*) and Cohen *et al.* (*14*). Figure 1 illustrates the design of the EDB, which was immersed in a temperature-controlled bath. Droplets of $(NH_4)_2SO_4$ test solution were generated by a piezoelectric droplet generator (Uni-Photon Inc. Model 201). A dc potential of up of 60 V was applied to the top and bottom electrodes, in order to balance the particle, while an ac potential (100 Hz, 250–500 V) was applied to the middle ring electrode to prevent lateral movement. A laser beam was used to irradiate the particle so that it could be observed with a microscope. (We note that this does not lead to significant heating of the particle.)

A charged particle inside the EDB experiences an electrostatic force due to the dc field, a time varying force due to the ac field, gravitational force, and a drag force caused by any relative movement of the ambient air. When the electrostatic force due to the dc voltage balances the weight and the drag force of the particle, it can be held stationary. When there is no air flow, the electrostatic force will be equal to the weight of the particle. The mass of the particle, $\boldsymbol{m}$, is then given by:

$$\boldsymbol{m} = qV_{dc}/gZ_0 \qquad (17)$$

where q is the electrostatic charge carried by the particle, V_{dc} (V) is the dc voltage required to balance the particle, g is the acceleration due to gravity, and Z_0 is the distance between the top and bottom electrodes. Assuming no loss of charge, the relative mass change of a particle undergoing evaporation or condensation can be determined by the dc voltages required to balance the particle before and after the change.

The relationship between water activity and the aqueous concentration of the droplet, for a fixed mass of solute, is studied by varying the relative humidity (RH) of the air within the balance. At equilibrium, the chemical potential of water in the vapor phase is equal to that in the liquid. The influence of surface tension on the vapor pressure (the Kelvin effect) can be neglected since the droplets used here are about 20 μm in diameter. Assuming ideal gas behavior, the water activity (a_1) within the droplet is given by

$$a_1 = p(H_2O)/p^\circ(H_2O) = RH \qquad (18)$$

where $p(H_2O)$ is the vapor pressure of water within the balance and $p^\circ(H_2O)$ the saturation vapor pressure of water at the same temperature.

Figure 2 shows the system for controlling and measuring temperature and relative humidity in the EDB. Nitrogen at 2 bar was used as a carrier gas in the experiment. Water vapor was introduced into the system by diverting part of the N_2 stream through a bubbler containing pure water. The dew point of the gas going to the EDB was controlled by adjusting the ratio of the gas flowing through to that bypassing the bubbler. The hygrometer (EG&G DewPrime Model 2000) requires an operational flow rate of about 1 $dm^3\ min^{-1}$ which is too high for keeping the particle trapped in the EDB. The moisturized N_2 stream was therefore divided into two: 100 $cm^3\ min^{-1}$ to the EDB and the rest to the hygrometer. All plumbing between the bubbler and temperature bath, including the dew point sensor, were enclosed and kept at a temperature 10 °C higher than the constant temperature bath in order to avoid condensation. Special precautions were also taken in the design of the EDB and the temperature bath to avoid water leaks and condensation of water vapor on the balance and the pipes. Thermal equilibrium was ensured by monitoring the temperature of the gas flowing out of the EDB in addition to that of the bath.

(b) Procedure. Test solutions were made up from reagent grade $(NH_4)_2SO_4$ and deionized water. Droplets injected into the EDB using the piezoelectric generator had an initial concentration of about 1.1 mol dm^{-3}. Measurements of the dc balancing voltage, at different relative humidities, were made for a series of particles at temperatures from 5 to 40 °C. In each case the relative humidity was varied between a maximum of approximately 80% to a lower limit (about 40%) beyond which particles evaporated to dryness. The precision of the dew point meter is ±0.2 °C, corresponding to an uncertainty in relative humidity of about 1%, and that of the digital thermocouple thermometer (reading the temperature of the EDB) is ±0.1

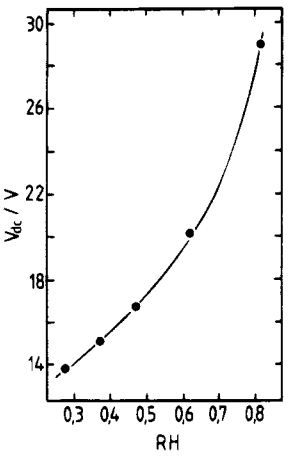

Figure 3. Measured dc voltages for the suspension of a pure aqueous H_2SO_4 particle at 25 °C (symbols), compared with values estimated by using the model of Clegg and Brimblecombe (*6*) to calculate the relationship between water activity and particle composition.

°C. The precision with which V_{dc} can be determined is limited by visual error, and is lowest for the smallest particles, but always better than 1%.

In some cases measurements were made, usually for different temperatures, using the same particle held in the EDB over periods of up to two and a half days. Comparisons of the results showed that some charge loss was occurring, later measurements requiring the highest overall V_{dc}. However, for measurements made with a single particle over a 24 h period the effect was negligible. Also, each set of determinations at a single temperature (made over a period of <11 h) was standardized individually. Thus, loss of particle charge is not thought to significantly affect our results.

As a test, measurements of V_{dc} were made for a pure aqueous H_2SO_4 particle from 81.74% to 27.52% relative humidity at 25 °C. These are compared in Figure 3 with theoretical predictions (*6*) based on isopiestic and vapor pressure data for bulk solutions. There is good agreement at all relative humidities, with deviations of only +1.2% to −1.9% in terms of the osmotic coefficient, ϕ.

(c) Results. Measured balancing voltages (V_{dc}) and water activities (a_1, equivalent to relative humidity) are listed in Table 1. Two sets of data from a previous study at 25 °C are included (*13*), as are some unpublished measurements obtained using a third instrument (*15*). Because each particle studied has a different charge and solute mass, V_{dc} values at each temperature have been normalized for comparability.

A reference state is required for the determination of solute molality from the measurements of V_{dc} that are obtained using the balance. There are two logical choices: a dry particle, or a droplet at low molality (high RH) for which other thermodynamic data are available which define the relationship with water activity. Tang and Munkelwitz (*11*) and Cohen *et al.* (*14*) found that the particles resulting from drying levitated electrolyte solution droplets may not be in the most thermodynamically stable state nor completely free of water. While droplets give a well-defined light scattering pattern, solid particles reflect and scatter light more irregularly, making it difficult to determine V_{dc} accurately. Therefore, Chan *et al.* (*13*), and more recently Tang and Munkelwitz (*11*), used droplets at high relative humidity (~80% RH) as reference states in studies of water activities of concentrated $(NH_4)_2SO_4$ and NH_4NO_3 droplets and obtained consistent results. The same approach is adopted here.

Table 1. Experimental Results

n^a	t/°C	a_1	$V_{dc}{}^b$/V	m/(mol kg^{-1})	n^a	t/°C	a_1	$V_{dc}{}^b$/V	m/(mol kg^{-1})
1	5	0.8010	17.594	5.68	6	25	0.7088	7.854	8.40
1	5	0.7617	15.908	6.82	6	25	0.7971	9.720	5.59
1	5	0.6588	13.651	9.34	6	25	0.6827	7.696	8.77
1	5	0.6125	12.688	11.09	6	25	0.5703	6.449	13.49
1	5	0.5645	11.862	13.21	6	25	0.5264	6.104	15.84
1	5	0.4646	10.633	18.46	6	25	0.4562	5.647	20.63
1	5	0.4180	10.172	21.70	6	25	0.8271	10.315	5.06
3	5	0.8475	20.169	4.52	6	25	0.3955	5.369	25.26
3	5	0.8005	17.509	5.73	7	25	0.5166	5.946	17.28
3	5	0.7447	15.552	7.12	7	25	0.8069	9.679	5.64
3	5	0.6485	13.284	9.94	7	25	0.7044	7.930	8.24
3	5	0.5433	11.669	13.83	7	25	0.6534	7.317	9.83
3	5	0.4464	10.462	19.54	7	25	0.5472	6.369	14.01
3	5	0.7502	15.529	7.15	7	25	0.5061	6.009	16.70
3	5	0.3980	9.900	24.19	7	25	0.4470	5.593	21.45
4	5	0.8296	18.965	5.00	3[c]	25	0.8092	9.650	5.65
4	5	0.7447	15.718	6.98	3[c]	25	0.7811	9.131	6.24
4	5	0.6678	13.596	9.43	3[c]	25	0.7572	8.685	6.85
4	5	0.5937	12.374	11.81	3[c]	25	0.6874	7.707	8.73
4	5	0.5391	11.354	14.97	3[c]	25	0.5970	6.761	11.86
6	5	0.5510	11.740	13.59	3[c]	25	0.5086	6.009	16.59
6	5	0.8236	18.579	5.17	5[c]	25	0.8046	9.607	5.73
6	5	0.7720	16.728	6.21	5[c]	25	0.7701	8.851	6.65
6	5	0.7392	15.407	7.26	5[c]	25	0.7079	8.009	8.10
6	5	0.6530	13.391	9.76	5[c]	25	0.6251	7.019	10.88
6	5	0.5978	12.377	11.80	5[c]	25	0.5302	6.279	14.65
6	5	0.5270	11.387	14.84	9[d]	25	0.803	9.51	5.81
6	5	0.4924	10.890	17.04	9[d]	25	0.790	9.31	6.04
6	5	0.4495	10.415	19.86	9[d]	25	0.763	8.68	6.87
6	5	0.3977	9.892	24.28	9[d]	25	0.738	8.08	7.92
5	10	0.4473	12.882	19.55	9[d]	25	0.519	6.09	15.96
5	10	0.4707	13.251	17.73	9[d]	25	0.578	6.59	12.72
5	10	0.5100	13.730	15.82	9[d]	25	0.637	7.16	10.32
5	10	0.5485	14.362	13.85	9[d]	25	0.683	7.68	8.81
5	10	0.5977	15.227	11.83	9[d]	25	0.708	7.88	8.34
5	10	0.6694	17.014	9.10	9[d]	25	0.740	8.46	7.22
5	10	0.6982	17.646	8.41	2	35	0.8247	15.716	5.21
5	10	0.7589	19.976	6.58	2	35	0.7616	13.727	6.62
5	10	0.8299	23.340	5.00	2	35	0.6742	11.705	9.15
5	10	0.8299	23.209	5.05	2	35	0.5757	10.074	13.22
2	15	0.3883	7.336	24.14	2	35	0.5236	9.422	16.08
2	15	0.4448	7.738	19.64	2	35	0.4668	8.781	20.41
2	15	0.5449	8.625	13.91	2	35	0.4206	8.461	23.59
2	15	0.6467	9.914	9.77	5	35	0.8103	15.155	5.54
2	15	0.7012	10.706	8.26	5	35	0.7503	13.306	7.03
2	15	0.7398	11.673	6.94	5	35	0.7123	12.314	8.21
2	15	0.8446	14.809	4.58	5	35	0.6683	11.574	9.38
1	15	0.4249	7.731	19.70	5	35	0.6303	11.004	10.54
1	15	0.4759	8.131	16.61	5	35	0.5977	10.476	11.91
1	15	0.5247	8.546	14.28	5	35	0.5306	9.528	15.53
1	15	0.5740	9.028	12.28	5	35	0.4788	9.070	18.20
1	15	0.5779	9.111	11.99	7	35	0.8383	16.489	4.81
1	15	0.6759	10.358	8.86	7	35	0.7393	12.976	7.38
1	15	0.7776	12.247	6.35	7	35	0.6435	11.182	10.15
1	15	0.8255	13.787	5.15	7	35	0.5228	9.385	16.27
1	25	0.6297	7.091	10.64	7	35	0.4746	8.864	19.73
1	25	0.7181	8.057	8.02	7	35	0.4982	9.132	17.79
1	25	0.7781	8.987	6.48	8	40	0.8144	38.020	5.47
1	25	0.5264	6.212	15.17	8	40	0.7032	30.013	8.59
1	25	0.4807	5.921	17.65	8	40	0.6500	27.566	10.40
1	25	0.4299	5.619	21.26	8	40	0.6037	26.132	11.87
1	25	0.8172	10.026	5.33	8	40	0.5508	24.775	13.69
2	25	0.8399	10.714	4.81	8	40	0.4990	22.799	17.65
2	25	0.7521	8.673	6.98	8	40	0.4488	21.634	21.27
2	25	0.6939	7.803	8.65					
2	25	0.6477	7.173	10.46					
2	25	0.5474	6.420	13.95					
2	25	0.4476	5.745	19.90					
2	25	0.3946	5.279	28.19					
4	25	0.8397	10.805	4.75					
4	25	0.7290	8.191	7.83					
4	25	0.6155	6.876	11.62					
4	25	0.5112	6.192	15.54					

[a] Particle number. [b] Listed values of V_{dc} at each temperature have been normalized. [c] Data for two particles measured by Chan *et al.* (*13*). [d] Unpublished results (*15*).

Molalities of the particles were obtained as follows. Isopiestic data for aqueous $(NH_4)_2SO_4$ are available at

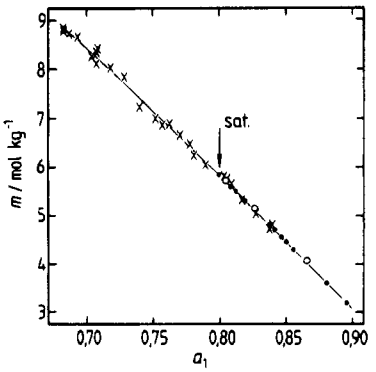

Figure 4. Standardization of EDB data at 25 °C. Symbols: (•) isopiestic data of Wishaw and Stokes (*16*), (○) isopiestic data of Filippov *et al.* (*17*), (×) EDB measurements. Line: fitted empirical equation (see section 3). The water activity (a_1) at which saturation occurs in bulk solutions is also indicated.

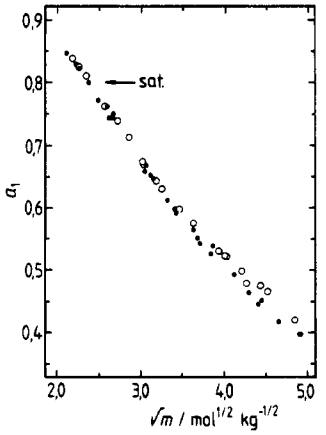

Figure 5. Water activities at 5 °C (•) and 35 °C (○), obtained from the EDB data (Table 1) for supersaturated droplets. The water activity (a_1) at which saturation in bulk solutions occurs is indicated.

298.15 K to 5.83 mol kg^{-1} ($a_1 = 0.800$) (*16*, *17*). For a_1 from about 0.9 to 0.7, the molality of $(NH_4)_2SO_4$ can be accurately represented using an empirical function of the form $m(NH_4)_2SO_4 = c_1 + c_2(1 - a_1)^{c_3}$. Also, since V_{dc} is proportional to total particle mass, it is related to molality by $m(NH_4)_2SO_4 = 1000/(V_{dc}/c_4 - M((NH_4)_2SO_4))$, where $M((NH_4)_2SO_4)$ (132.134 g mol^{-1}) is the molar mass of the solute and c_4 a constant to be determined empirically. All 25 °C balance data were standardized by fitting the two equations simultaneously to the isopiestic data for $a_1 < 0.9$ and balance data for $a_1 > 0.7$. The result is shown in Figure 4. Data for all other temperatures were standardized in a similar way, though using balance data only for $a_1 > 0.8$, and also taking into account the dependence of a_1 on temperature in the case of the isopiestic measurements. This effect is, however, small compared to the uncertainties in the balance measurements. Molalities of $(NH_4)_2SO_4$ for all particles are listed in Table 1, and are plotted with water activity for 5 and 35 °C in Figure 5. Although the data are scattered, a trend of increasing water activity with temperature is apparent at the highest molalities.

4. Literature Data

Sources of available thermodynamic data for the system $(NH_4)_2SO_4$–H_2O are listed in Table 2. One of the most significant features, for the present analysis, is the paucity of thermal measurements which enable the variation of solvent and solute activities with temperature (at subsaturated concentrations) to be estimated. The data are briefly reviewed below.

(a) Freezing Point Depression. This quantity yields the solvent activity at the freezing point of the solution (*18*, *19*). Here we use the following expression for the water activity (a_1) in terms of the freezing point depression ϑ (°C), adapted from Klotz (*18*) and given by Carslaw *et al.* (*20*):

$$\log(a_1) = -4.2091 \times 10^{-3}\vartheta - 0.2152 \times 10^{-5}\vartheta^2 + 0.3233 \times 10^{-7}\vartheta^3 + 0.3446 \times 10^{-9}\vartheta^4 + 0.1758 \times 10^{-11}\vartheta^5 + 0.765 \times 10^{-14}\vartheta^6 \quad (19)$$

It has been noted by Clegg and Brimblecombe (*7*) that osmotic coefficients of aqueous $(NH_4)_2SO_4$, derived from freezing point data (*21*), deviate from the Debye–Hückel limiting law slope at very low molalities. Consequently, all freezing point data were rejected in our previous analysis (*7*) of osmotic and activity coefficients. The effect may be due to the incorporation of solute ions into the precipitating ice, as is found in the cases of aqueous NH_4Cl (*22*) and aqueous H_2SO_4 (*6*, *23*). However, for H_2SO_4 at least, the problem appears to be restricted to relatively low molalities (below about 0.1 mol kg^{-1}). Freezing point data for aqueous $(NH_4)_2SO_4$ were therefore considered for inclusion in the present analysis, since the available data can be used to obtain a_1 at higher molalities up to the eutectic point (~5 mol kg^{-1}). Measured freezing point depressions from sources listed in Table 2 are shown in Figure 6. The data are quite scattered—which becomes even more apparent when they are plotted as osmotic coefficients at the freezing temperature of the solution—and so were not used in our analysis. However, freezing points calculated using the completed model (section 5), and shown in Figure 6, are consistent with the measurements.

(b) Boiling Points. Water activities (a_1) at the boiling point of the solution are calculated from the equation $a_1 = p(H_2O)/p°(H_2O)$, where $p°(H_2O)$ is the vapor pressure of pure water at the boiling temperature and $p(H_2O)$, the partial pressure of water, is equal to the total pressure of the system. The above relationship assumes that partial pressure is equivalent to fugacity. Test calculations using an equation of state to estimate fugacity coefficients showed that this was a satisfactory approximation. Values of $p°(H_2O)$ were obtained using the equation of state of Hill (*24*).

Five sources of boiling point elevations are listed in Table 2. The values of Gerlach (data set 41) were presented only as smoothed concentrations as a function of temperature, and it is unclear how they were obtained. The data were also found to be discordant with those of other researchers, and were therefore rejected. Johnston (data set 43) noted that in his experiments the boiling temperature of pure water was dependent upon the amount of heat applied, though this was not so for the $(NH_4)_2SO_4$ solutions (*25*). Plots of boiling point elevation against molality for Johnston's data (*25*) indeed show systematic displacements consistent with different values of the boiling point of pure water (note that Johnston took into account the effect of variations of atmospheric pressure upon his results). All the measurements of Johnston (made close to sea level) were therefore adjusted to be consistent with a single boiling point of pure water of 373.15 K. This was done by adding a Δ (K) to each data set, bringing the measurements into optimum agreement with each other and converging to a boiling point elevation of zero for pure water. The most extensive measurements are those of Buchanan (data set 42), for six pressures corresponding to boiling points of pure water ranging from 364.31 K (91.3 °C) to 373.43 K (100.28 °C). Data are plotted in Figure 7 as boiling temperature

Table 2. Availability of Thermodynamic Data for Aqueous $(NH_4)_2SO_4$ Solutions

$m((NH_4)_2SO_4)$	t/°C	type[a]	N	ref[b]
0.76–4.92	−20.4 to −2.8	satd (ice)	1	40
0.0009–1.21	−4.02 to −0.005	satd (ice)	2	21
0.050–1.527	−5.13 to −0.24	satd (ice)	3	41
0.303–2.72	−9.7 to −1.1	satd (ice)	4	28
0.841–5.76	−17 to +19	satd (ice, AS)	5	28
2.18–5.02	−18.3 to −7.1	satd (ice, AS)	6	28
0.254–7.70	−18.5 to +100	satd (ice, AS)	7	28
0.253–5.73	−18.85 to +29	satd (ice, AS)	8	28
0.382–6.14	−18.8 to +42.4	satd (ice, AS)	9	28
5.57–5.62	9–15	satd (AS)	10	28
5.35–6.93	0–70	satd (AS)	11	28
5.67–6.46	16.5–51.8	satd (AS)	12	28
5.34–8.13	0.0 −108.9	satd (AS)	13	28
9.07–29.53	138–410	satd (AS)	14	28
7.908	107.03	satd (AS)	15	28
5.00–6.55	−19.05 to +55.7	satd (AS)	16	42
5.805–7.75	25–105	satd (AS)	17	43
5.48–6.79	0–60	satd (AS)	18	44
5.76	19.0	satd (AS)	19	45
5.76–7.60	25–97	satd (AS)	20	46
5.87–6.58	25–60	satd (AS)	21	47
4.993	−18.5	eutectic	22	48
1.756–2.697	25	iso	23	49
0.129–5.83	25	iso	24	16
0.583–5.714	25	iso	25	17
5.797–36.33	~24	vp (balance)	26	37
4.194–18.86	~20	vp (balance)	27	38
3.53–28.82	25	vp (balance)	28	11
5.66–16.60	~25	vp (balance)	29	13
5.80–15.9	25	vp (balance)[c]	30	15
4.52–28.19	5–40	vp (balance)	31	this study
0–3.096	31.97–100.09	vp[d]	32	28
5.82, 6.63	25–70	vp	33	26
5.90	35–50	vp[e]	34	27
satd soln	10–50	vp	35	28
satd soln	10.97–35.31	vp	36	50
satd soln	10.3–33.8	vp	37	29
satd soln	19–30	vp	38	51
satd soln[f]	14.8–33.1	vp	39	52
satd soln	0.39–47.96	vp	40	53
0–8.725	100–108.2	bp[g]	41	28
0–8.809	91.16–108.09	bp	42	54
0.025–7.33[h]	100.04–106.26	bp	43	25
8.133	108.9	bp[g]	44	28
8.046	108.5	bp (satd)[i]	45	48
0–5.55	25	$\Delta_f H°$[j]	46	33
0.0347–0.555	20	$\Delta_{sol}H$[k]	47	55
0.1388	18–88.2	$\Delta_{sol}H$[k]	48	55
0.756–4.54	10–60	C_p[l]	49	30
24.6–40 wt %	23–92	C_p[m]	50	31
0.28–3.70	19–21	C_p[n]	51	32

[a] Data types are as follows: satd, solution saturated with respect to ice or $(NH_4)_2SO_4$ (AS); iso, isopiestic measurement; vp, direct vapor pressure or EDB (balance) measurement; bp, boiling point; $\Delta_f H°$, tabulated enthalpy of formation; $\Delta_{sol}H$, enthalpy of solution; C_p, heat capacity or specific heat. There are some additional sources of solubility data not used in the present analysis: Britton (*56*) (25 °C), Weston (*57*) (25–60 °C), Caven and Mitchell (*58*) (25–61 °C), Schreinemakers (*59*, *60*) (30 °C), and a few others given in early editions of the *Landolt-Börnstein Tables*. [b] Sources of the experimental data compiled by Timmermans (*28*) are as follows for each data set N: 4, Rudorf (1872); 5, Guthrie (1876); 6, Rodebush (1918); 7, Ishikawa and Murooka (1929, 1933); 8, Bergman and Sholokhovich (1942); 9, Vasilenko (1948); 10, Bodlander (1891); 11, de Waal (1910); 12, Lattey (1923); 13, Mulder (1866); 14, Benrath *et al.* (1937); 15, Buchanan (1899); 32, Tammann (1885); 35, Adams and Merz (1929); 41, Gerlach (1886); 44, Mulder (1866). [c] Unpublished data. [d] Timmermans (*28*) incorrectly gives the concentrations measured by Tammann (*61*) as being in weight percent, rather than g of solute/100 g of H_2O. [e] Chatterji and Rastogi (*27*) list the measured $p(H_2O)$ and $p°(H_2O)$, in addition to water activity. For several salts, including $(NH_4)_2SO_4$, the water activities do not correspond to $p(H_2O)/p°(H_2O)$. Tabulated a_1 are consistent with the authors' characterization of the $(NH_4)_2SO_4$ water activities being either invariant with temperature, or having a small negative trend. However, values of $p(H_2O)/p°(H_2O)$ tend to *increase* with temperature. [f] As tabulated by Apelblat (*50*). [g] Total pressure not given. [h] Data tabulated for normalities were not used, but some results given in Johnston's Figure 3 were included. [i] Boiling point of a solution saturated with respect to $(NH_4)_2SO_4$. This value and the composition and temperature of the eutectic point are evaluations from literature data. [j] These enthalpies of formation (from which enthalpies of solution were calculated) were originally estimated by Rossini *et al.* (*62*, *63*), from the work of the following authors: Bouzat (1903), Roth and Zeumer (1931), and Thomsen (1882–1886). An earlier evaluation appears in the *International Critical Tables of Numerical Data, Physics, Chemistry and Technology (64)*, for 0.134–5.55 mol kg^{-1}, based on the same data of Bouzat (1903) and Thomsen (1882–1886), and the work of Berthelot (1873). [k] Integral enthalpies of solution at 20 °C are from the work of Roth and Zeumer (1931). Values from 18 to 88.2 °C, for a single concentration, are from the results of Roth and Zeumer (1931), Thomsen (1878), and Cappellina and Napolitano (1967). The last reference appears to have been given incorrectly in the *Landolt-Börnstein Tables*, and should be *Ann. Chim.* **1967**, *57*, 1087. [l] Data presented graphically. [m] Data presented graphically. Values at 25 °C were estimated for three molalities from Schneider *et al.*'s Figure 2. [n] Data from Marignac (1876). An equation is presented in the *International Critical Tables of Numerical Data, Physics, Chemistry and Technology (64)*, for the same range of molality, also based upon the work of Marignac (1876) and that of Thomsen (1871). This equation reproduces essentially the same values as are listed in the *Landolt-Börnstein Tables* (*32*).

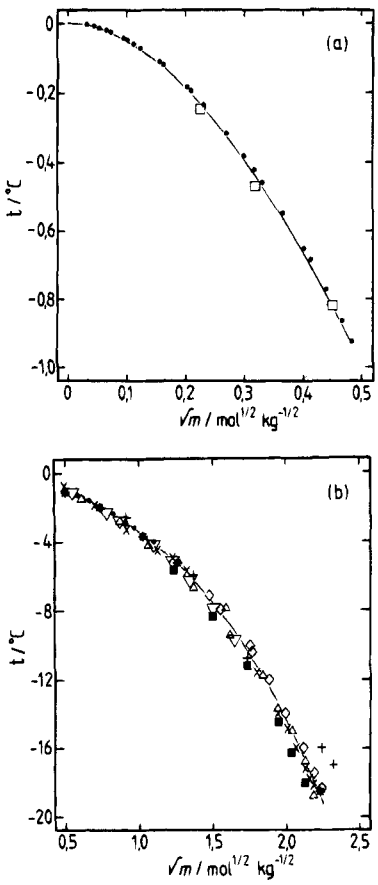

Figure 6. Freezing points of pure aqueous $(NH_4)_2SO_4$ solutions, plotted against the square root of molality ($\sqrt{m}$/mol$^{1/2}$ kg$^{-1/2}$). Sources of data (N in Table 2) are as follows: (■) 1, (•) 2, (□) 3, (▽) 4, (+) 5, (◇) 6, (*) 7, (×) 8, (△) 9. Lines are calculated values, using the final model (section 5) together with eq 19.

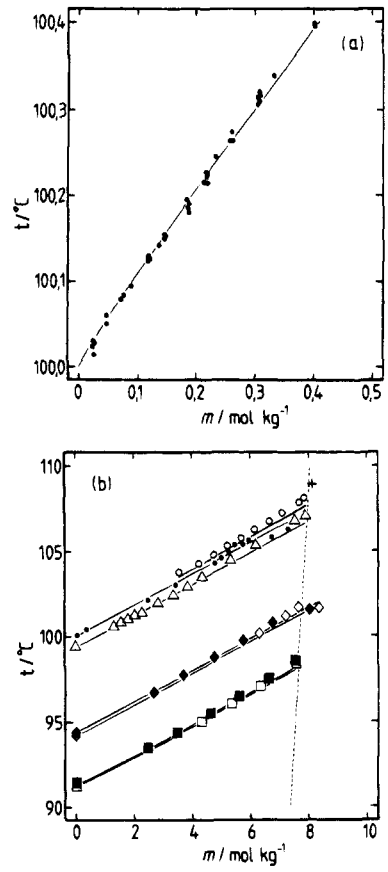

Figure 7. Boiling points of pure aqueous $(NH_4)_2SO_4$ solutions, plotted against molality (m/mol kg^{-1}). Sources of data are as follows: (a) low molality measurements of Johnston (N = 43); (b) (+) Mulder (N = 44), (•) Johnston (N = 43); (other symbols) Buchanan (N = 42). In part b the boiling points of pure water at the experimental pressures are as follows: (○) 100.28 °C, (•) 100 °C, (+) 100 °C, (△) 99.4 °C, (♦) 94.41 °C, (◇) 94.24 °C, (■) 91.3 °C, (□) 91.16 °C. Full lines are calculated values, using the final model (section 5) together with $p°(H_2O)$ derived from Hill's equation of state (*24*). The dotted line is the saturation curve of aqueous $(NH_4)_2SO_4$.

against $(NH_4)_2SO_4$ molality. These results, when compared with other isopiestic data at 298.15 K, show that the water activity at the boiling temperature is higher than at 298.15 K. The boiling point measurements have been included in our analysis, as they allow the variation of a_1 with temperature to be constrained for $(NH_4)_2SO_4$ concentrations below those measured by the EDB. Boiling points calculated using the final model are also shown in Figure 7.

(c) Vapor Pressure Measurements. Partial pressures of water above aqueous $(NH_4)_2SO_4$ solutions (below saturation) have been measured by Tammann (data set 32), Emmons and Hahn (data set 33 (*26*)), and Chatterji and Rastogi (data set 34 (*27*)). The latter study is of solutions supersaturated by a very small amount. The partial pressures of Emmons and Hahn for 5.82 mol kg^{-1} $(NH_4)_2SO_4$ (25–60 °C) and 6.63 mol kg^{-1} (55–70 °C) were converted to a_1 using the authors' listed $p°(H_2O)$. The measurements of Tammann were similarly converted, using the $p°(H_2O)$ given by Timmermans (*28*) (see also note *d* in Table 2). Values of a_1 listed by Chatterji and Rastogi (*26*) were taken directly (but see note *e* in Table 2). In view of the relatively small change in water activity with temperature found for aqueous $(NH_4)_2SO_4$ at moderate concentrations, compared with the uncertainties inherent in vapor pressure measurements, these data have not been used to constrain our treatment of the thermodynamics of aqueous $(NH_4)_2SO_4$. However, they are compared with water activities calculated using the model in Figure 8. The data of Emmons and Hahn and of Chatterji and Rastogi do not agree with the model, even close to 298.15 K where the water activity is known very accurately, and are considered to be in error. However, the earlier measurements of Tammann (data set 32) agree well with the model calculations at all temperatures.

(d) Enthalpies of Solution. The most comprehensive evaluation of enthalpies of solution (data set 46 in Table 2, 10 values to 5.55 mol kg^{-1}) is based upon three studies, all of which were carried out more than 60 years ago; see note *j* of Table 2. There appear to be no more recent measurements, with the exception of the work of Cappellina and Napolitano (data set 48 in Table 2), which is for 0.1388 mol kg^{-1} $(NH_4)_2SO_4$ over a range of temperatures. As found by Tang and Munkelwitz (*29*), the value of $\Delta_{sol}H$ for 5.55 mol kg^{-1} $(NH_4)_2SO_4$, from data set 46, is consistent with measured water vapor pressures over saturated solutions of $(NH_4)_2SO_4$, and these enthalpies of solution are therefore adopted in the present work. They are shown in Figure 9 as $^{\phi}L$, together with fitted values calculated using the completed thermodynamic model. There is only moderate agreement, and the reason for the differences is unclear. New measurements of enthalpies of dilution of aqueous $(NH_4)_2SO_4$ would be worthwhile.

(e) Heat Capacities. Three sources of heat capacity data are listed in Table 2. The results of Sukhatme and Saikhedkar (*30*) (data set 49) and Schneider *et al.* (*31*) (data set 50) are presented only in graphical form, while those listed in the *Landolt-Börnstein Tables* (*32*) (data set 51) are an evaluation of very early measurements. We have

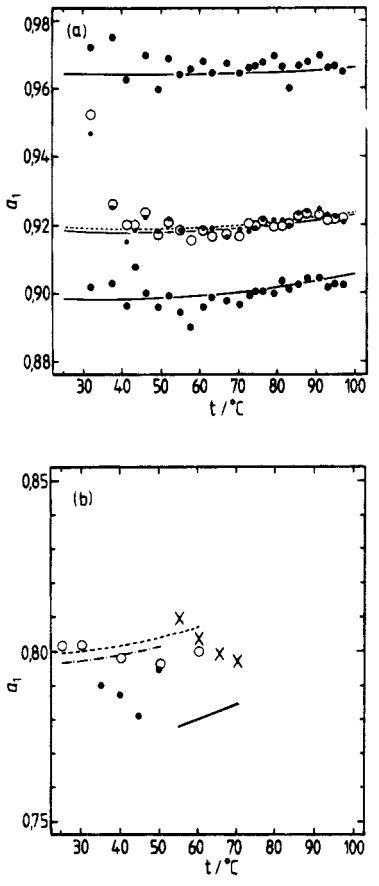

Figure 8. Water activities (a_1) of aqueous $(NH_4)_2SO_4$, from direct vapor pressure determinations, as a function of temperature: (a) data of Tammann ($N = 32$) for four molalities (m): (●) 1.054 mol kg^{-1} (uppermost portion of the graph), (○) 2.489 mol kg^{-1}, (•) 2.513 mol kg^{-1}, (●) 3.096 mol kg^{-1} (lower portion of graph); (b) data of Emmons and Hahn ($N = 33$) for 5.820 and 6.630 mol kg^{-1}, and Chatterji and Rastogi ($N = 34$) for 5.903 mol kg^{-1}. Symbols in (b): (○) 5.820 mol kg^{-1}, (●) 5.903 mol kg^{-1}, (×) 6.630 mol kg^{-1}. All lines were calculated using the thermodynamic model described in section 5. In (b) the dashed line is for 5.820 mol kg^{-1}, the dashed–dotted line is for 5.903 mol kg^{-1}, and the solid line is for 6.630 mol kg^{-1}.

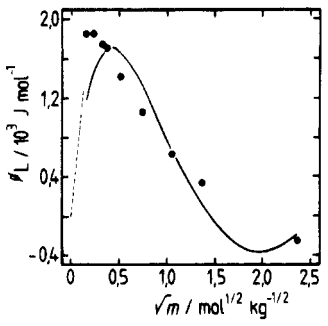

Figure 9. Enthalpies of dilution ($^{\phi}L$/J mol^{-1}) of aqueous $(NH_4)_2SO_4$ at 298.15 K: symbols, data set 46; solid line, fitted model (section 5); dotted line, limiting slope, equivalent to the first term in eq 7.

calculated an additional value of $^{\phi}C_p$ equal to −30.5 J mol^{-1} K^{-1} for 0.1388 mol kg^{-1} at 298.15 K from tabulated enthalpies of solution (data set 48 in Table 2) and a specific heats of $(NH_4)_2SO_{4(cr)}$ equal to 187.49 J mol^{-1} K^{-1} (*33*). Apparent molar heat capacities were calculated from specific heats listed in the *Landolt-Börnstein Tables* (*32*) assuming units of cal_{20} g^{-1} K^{-1} (1 J = 0.2391$_8$ cal_{20} (*34*)), and from data sets 49 and 50 (which are in joules) using heat capacities of water taken from the *CRC Handbook of Chemistry and Physics* (*35*). The most recent estimate of

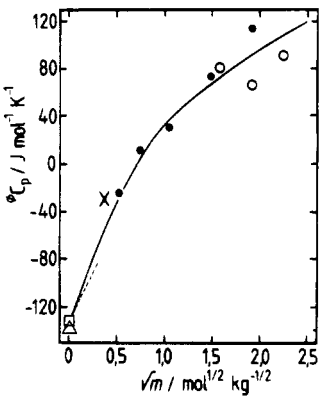

Figure 10. Apparent molar heat capacities ($^{\phi}C_p$/J mol^{-1} K^{-1}) of aqueous $(NH_4)_2SO_4$ at 298.15 K. Symbols: (□) $^{\phi}C_p^{\circ}$ from Wagman *et al.* (*33*), (△) $^{\phi}C_p^{\circ}$ from Desnoyers *et al.* (*36*), (×) data set 48, (○) data set 50, (●) data set 51. Lines: (solid) fitted model (section 5); (dotted) limiting slope, equivalent to the second term in eq 8.

$^{\phi}C_p^{\circ}$ for aqueous $(NH_4)_2SO_4$ is −139 J mol^{-1} K^{-1} (*36*), which agrees well with the −133.1 J mol^{-1} K^{-1} tabulated by Wagman *et al.* (*33*).

Initial comparisons of the data showed that the results of Sukhatme and Saikhedkar (*30*) (data set 49) were grossly discordant with other measurements, and are probably in error. (We note that heat capacities of aqueous NH_4NO_3, measured by these authors (*30*), also deviate greatly from literature data.) The results of Sukhatme and Saikhedkar (*30*) were therefore rejected. However, the other measurements were used in the correlation of thermodynamic properties described in the following section.

Data for 298.15 K °C, neglecting the fact that the Landolt-Börnstein values are for a few degrees lower, are shown in Figure 10 together with values calculated using the fitted thermodynamic model (section 5). There is good agreement.

5. Analysis

One of the aims of the present study is to determine the thermal properties of aqueous $(NH_4)_2SO_4$, to high concentration, using both the EDB measurements given in Table 1 and literature data referenced in Table 2. From Figure 5 it is clear that the magnitude of the variation of a_1 over the range 5–35 °C is close to the precision of the balance measurements, even at the highest molalities where the change is greatest. Nonetheless, it is still considered worthwhile to obtain estimates of enthalpies and heat capacities, and this is done below.

(a) Thermal Properties. Partial molar enthalpies of water (L_1, at 298.15 K) were first derived from the EDB data as follows. First, it was assumed that, over the range of temperature of the balance measurements, the change in partial molar enthalpies with temperature could be neglected (i.e., $J_1 = 0$). This allows L_1 to be calculated using eq 12 for each measurement for which $T \neq 298.15$ K. Since the EDB data are all at different molalities, corresponding values of a_1 at 298.15 K are required. These were obtained by fitting an equation of the form $\ln(a_1 - (298.15\ \text{K})) = a + bm^c$ to the EDB data from 6.3 to 25 mol kg^{-1}. Estimates of L_1 obtained in this way were then fitted, together with values of $^{\phi}L$ at low molality shown in Figure 9, using eqs 7 and 13. The result is shown in Figure 11, and fitted model parameters ($B^L_{NH_4SO_4}$, $B^{1L}_{NH_4SO_4}$, W^L_{1,NH_4SO_4}, U^L_{1,NH_4SO_4}, and V^L_{1,NH_4SO_4}) are listed in Table 3. Note that some values of L_1 that deviated greatly from the general trend were rejected, and are not included in the figure. While the values of L_1 derived from the balance

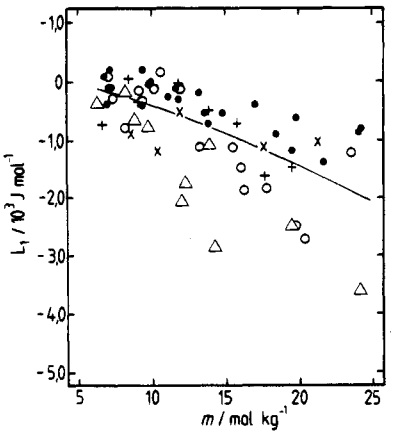

Figure 11. Partial molar enthalpies of water (L_1/J mol^{-1}) in aqueous $(NH_4)_2SO_4$ at 298.15 K, determined from EDB data in Table 1. Symbols indicate values derived from measurements at five temperatures, as follows: (●) 5 °C, (+) 10 °C, (△) 15 °C, (○) 35 °C, (×) 40 °C. The solid line represents the fitted model (section 5).

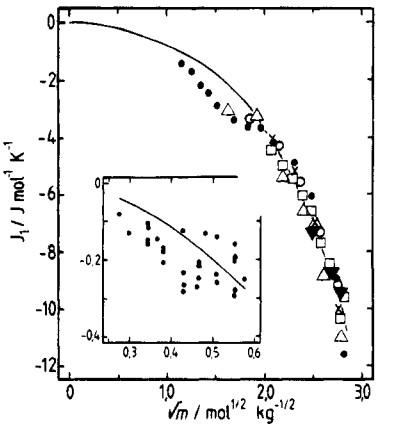

Figure 12. Partial molar heat capacities of water (J_1/J mol^{-1} K^{-1}) in aqueous $(NH_4)_2SO_4$ at 298.15 K, determined from boiling point elevations of Buchanan (N = 42 in Table 2) and (inset) Johnston (N = 43). Symbols (main plot) indicate measurements at six different pressures, for which the boiling temperatures of pure water are as follows: (□) 100.28 °C, (●) 99.40 °C, (△) 94.41 °C, (▼) 94.24 °C, (○) 91.30 °C, (×) 91.16 °C. The inset shows the data of Johnston for a nominal boiling temperature of 100 °C. Lines show the fitted model (eqs 8 and 14).

data are scattered, as expected, the tendency to negative partial molar enthalpies with increasing molality is clear, and the fitted model provides reasonable estimates of solution behavior for both subsaturated (Figure 9) and supersaturated conditions.

(b) Heat Capacities. Apparent molar heat capacities ($^{\phi}C_p$) for molalities to 4.54 mol kg^{-1} were discussed in section 4. Boiling point elevations yield the water activity at the boiling temperature of the solution. Partial molar heat capacities of water (J_1, to 8.8 mol kg^{-1}) were derived from these data by first assuming J_1 to be invariant with temperature from 298.15 K to the boiling points, and then applying eq 12 together with values of L_1 obtained using eqs 7 and 13. Values of a_1 at 298.15 K were based upon isopiestic and EDB data for that temperature. The combined data set ($^{\phi}C_p$ and J_1) was then fitted using eq 8 (with $^{\phi}C_p^{\circ}$ set to −133.1 J mol^{-1} K^{-1}) together with eq 14, taking care to achieve a reasonable extrapolation to molalities beyond the upper limit of the boiling point data. The result is shown in Figure 10 for the $^{\phi}C_p$ measurements and in Figure 12 for the partial molar heat capacities. There is reasonable agreement for both sets of measurements. Parameters for the fitted model are given in Table 3.

Finally, as a test of consistency the calculation of L_1 from the EDB data was repeated, this time including the values of J_1 just obtained. The effect was to slightly reduce the degree of scatter shown in Figure 11, in particular bringing values for 278.15 and 308.15 K closer to the fitted line. No revision of the original fit was judged necessary.

(c) Osmotic Coefficients at 298.15 K. For practical applications, we have fitted eq 4 to osmotic coefficients at 298.15 K from both isopiestic data and balance measurements from Table 1 (with some outlying points, which appeared to be in error, removed). The result in shown in Figure 13 in terms of the molal osmotic coefficient ϕ, with parameters for the fitted model given in Table 3. While some systematic deviations from the measurements are apparent, the result is satisfactory overall, especially when variations between available sets of EDB measurements are taken into account (see section 6).

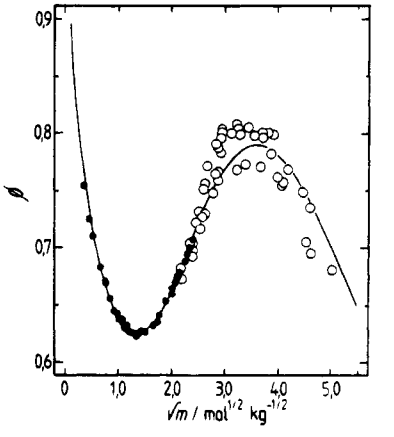

Figure 13. Molal osmotic coefficients (ϕ) at 298.15 K. Symbols are as follows: (●) isopiestic data (N = 24 and 25 in Table 2), (○) EDB measurements from Table 1. The line indicates values from the fitted model (eqs 3b and 4).

Table 3. Fitted Activity Coefficient Model Parameters at 298.15 K[a]

parameter	value	parameter	value	parameter	value
$B_{NH_4SO_4}$	13.99385	$B^L_{NH_4SO_4}$	0.0	$B^J_{NH_4SO_4}$	−0.021032
$B^1_{NH_4SO_4}$	−17.13243	$B^{1,L}_{NH_4SO_4}$	0.84618	$B^{1,J}_{NH_4SO_4}$	0.0046881
W_{1,NH_4SO_4}	−1.904921	W^L_{1,NH_4SO_4}	0.079118	W^J_{1,NH_4SO_4}	0.00064804
U_{1,NH_4SO_4}	2.125957	U^L_{1,NH_4SO_4}	−0.0071602	U^J_{1,NH_4SO_4}	0.00025844
V_{1,NH_4SO_4}	−2.291087	V^L_{1,NH_4SO_4}	−0.037725	V^J_{1,NH_4SO_4}	−0.00043965
$\alpha_{NH_4SO_4}$	13.0				
$\alpha^1_{NH_4SO_4}$	1.50				

[a] Both $\alpha_{NH_4SO_4}$ and $\alpha^1_{NH_4SO_4}$ are invariant with temperature. Values of parameters P (first column, used in eqs 4–6) and P^L (eq 7) at temperatures other than 298.15 K are obtained by integration, using the relationships given in eqs 9 and 10. (The second differentials with respect to temperature of each parameter P, which can be derived from $\{P^L, P^J\}$ pairs above using eq 10, are treated as being invariant with temperature.)

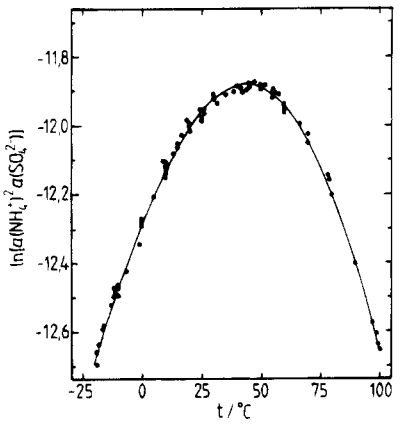

Figure 14. Logarithm of the equilibrium constant (K_s) (equivalent to $a(NH_4^+)^2a(SO_4^{2-})$) for saturation of solutions with respect to $(NH_4)_2SO_{4(cr)}$. Symbols indicate values calculated using measured solubilities and eqs 5 and 6, with parameters given in Table 3; the line indicates values from eq 20.

(d) $(NH_4)_2SO_4$ Solubility. Many measurements of this quantity have been made, and the 22 studies referred to in Table 2 are unlikely to form a complete list. The solubility of $(NH_4)_2SO_4$ varies by only about 3 mol kg^{-1} over a temperature range of >100 °C, from the eutectic point at 5.00 mol kg^{-1} and 254.21 K to the boiling point at about 380 K and 8 mol kg^{-1}. Calculated activity products of aqueous $(NH_4)_2SO_4$, defined in eq 16 and using eqs 5 and 6 to obtain the activity coefficients of the ions, are shown in Figure 14. The equilibrium constant K_s on a mole fraction basis (eq 16) is given by the following equation:

$$\ln(K_s) = -1102.015 + 23931.46/(T/\mathrm{K}) + 197.3493 \ln(T/\mathrm{K}) - 0.384466(T/\mathrm{K}) \quad (20)$$

where T is temperature. At 298.15 K, the value of K (6.39 × 10^{-6}) agrees to within 3.1% with that adopted previously (*7*).

6. Comparisons and Applications

(a) Other Data for Supersaturated Aqueous $(NH_4)_2SO_4$. In addition to the EDB measurements of Chan *et al.* (*13*) (data set 29) and Wyslouzil (*15*) (data set 30) included in our analysis, water vapor pressures of supersaturated solutions have also been measured by Spann (*37*) (data set 26) and by Tang and Munkelwitz (*11*) (data set 28). The results of the former study, which was made at room temperature, were included in a recent application of the present thermodynamic model to the system $(NH_4)_2SO_4$–H_2SO_4–H_2O (*7*). Water activities and osmotic coefficients obtained by Tang and Munkelwitz (*11*) and by Spann (*37*) at 298.15 K are compared with those from the present study in Figure 15. In terms of water activity the difference between our results and those of Tang and Munkelwitz is small. The data of Spann yield higher solute molalities, for a given relative humidity, than both other sets of measurements. A notable feature (Figure 15b) is the peak in ϕ at approximately 10 mol kg^{-1}, which is lower for the results of both Tang and Munkelwitz and Spann than found in the present study—the small difference (~0.05 in ϕ) corresponding to a change of about 0.017 in water activity. Cohen's measurements (*38*) (data set 27), which were obtained on an instrument similar to that of Chan *et al.* (*13*), agree with the higher values of ϕ obtained by us and by Wyslouzil (*15*). The reason for the differences shown in Figure 15 is unclear, though we note that both Tang and Munkelwitz (*11*) and Spann (*37*) used balances with evacuated chambers into which water vapor was introduced and pressure measured directly. This may be responsible for the high degree of precision that Tang and Munkelwitz in particular were able to achieve, but should not lead to different results overall. Loss of charge from the suspended particle may be a factor, although it was not thought to be significant in the present case and has not been noted by either Tang and Munkelwitz (*11*) or Spann (*37*) as a problem.

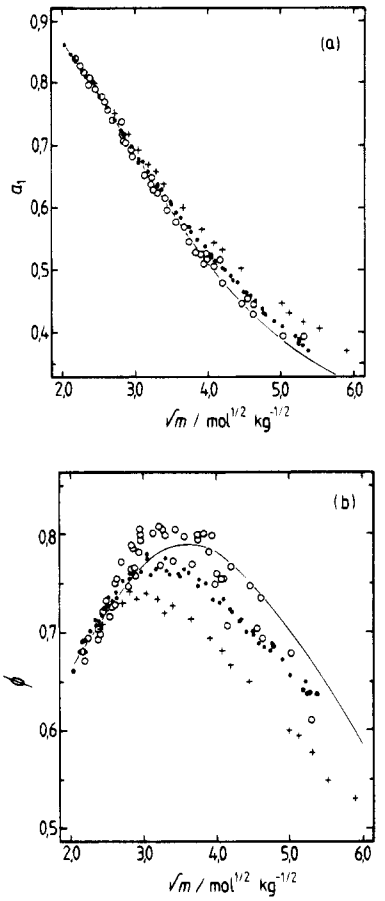

Figure 15. A comparison of water activities (in a) and osmotic coefficients (in b) of supersaturated aqueous $(NH_4)_2SO_4$ at 298.15 K from different sources: (○) this study, (●) Tang and Munkelwitz (*11*) (N = 28), (+) Spann (*37*) (N = 26). For clarity, some points have been omitted at low molalities.

In the present study the use only of EDB measurements (data sets 29–31) that are consistent with one another is justified for the purpose of estimating the variation of thermodynamic properties with temperature. The comparison with other data in Figure 15 shows that, for supersaturated solutions, there remains a small degree of uncertainty in the relationship between water activity and composition at 298.15 K. However, for practical applications such as calculations of the behavior of atmospheric aerosols, this is unlikely to be significant.

(b) Vapor Pressures above Saturated Aqueous $(NH_4)_2SO_4$. Tang and Munkelwitz (*29*) have shown that, for a saturated solution in equilibrium with the vapor phase, the following relationship applies between the water activity of the solution and the integral enthalpy of solution $\Delta_{sol}H$ (J mol^{-1}):

$$\partial \ln(a_1)/\partial T = -n\Delta_{sol}H/(RT^2) \quad (21)$$

where T is temperature, R (8.3144 J mol^{-1} K^{-1}) is the gas constant, and n is the salt solubility in moles of solute per mole of water. Water vapor pressures above solutions saturated with respect to $(NH_4)_2SO_4$ have been determined

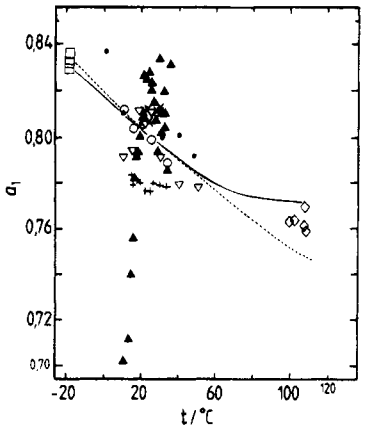

Figure 16. Water activities of saturated solutions of aqueous $(NH_4)_2SO_4$. Symbols are measured values from the following data sets N in Table 2: (□) 5, 6, 8, (▽) 35, (▲) 36, (○) 37, (×) 38, (+) 39, (●) 40, (◇) estimated from boiling point measurements (see text). The full line indicates values calculated using the thermodynamic model together with measured solubilities; the dotted line indicates values calculated by integration of eq 21.

by several authors (data sets 35–40 in Table 2). We have calculated a_1 from the vapor pressures, using Hill's equation of state to obtain $p°(H_2O)$, and the results are shown in Figure 16 for a range of temperatures. We have added values calculated from the measured eutectic point, and estimates for saturated solutions at their boiling points which were obtained by extrapolating measured boiling point elevations from data set 42 to the saturation molality. Also shown in the figure are, first, water activities calculated from the integration of eq 21 using a constant value of $\Delta_{sol}H$ (6.318 kJ mol^{-1} for 5.55 mol kg^{-1} $(NH_4)_2SO_4$ at 298.15 K (*33*)) and a_1(298.15 K) equal to 0.800. While these agree quite well with several of the existing sets of measurements from about 0 to 50 °C, as noted by Tang and Munkelwitz (*29*), at high temperature they deviate from the water activities obtained from boiling point data. Second, we show a_1 calculated using the fitted model, which effectively includes the variation of $\Delta_{sol}H$ with T. In this case, the predicted water activities for the saturated boiling mixtures are about 0.005 higher than the values estimated from measurements, while the predicted water activity at the eutectic point is little changed. Overall, the comparison suggests that the change in $(NH_4)_2SO_4$ solubility with temperature is the most important factor controlling the variation of a_1. Difficulties in obtaining a saturated solution may be responsible for the high degree of scatter of the data shown in Figure 16.

(c) Multicomponent Solutions containing NH_4^+ and SO_4^{2-}. Estimation of the properties of solution mixtures, for example $(NH_4)_2SO_4$–H_2SO_4–H_2O (*7*), requires the use of thermodynamic models (*5*, *39*). The parameters in Table 3 enable NH_4^+–SO_4^{2-} interactions to be calculated as functions of temperature to very high concentration—at least 25 mol kg^{-1} using the mole-fraction-based equations presented here. Extension of the model treatment of the system $(NH_4)_2SO_4$–H_2SO_4–H_2O (*7*) to temperatures other than 298.15 K is straightforward, as H_2SO_4–H_2O has already been parameterized using the model for 180 < T < 328 K. However, minor revisions to published parameters for 298.15 K will be necessary as activity coefficients for pure aqueous $(NH_4)_2SO_4$ now differ from those given previously, which were based only on Spann's results (*37*) for supersaturated solutions. These revisions will be given in a later paper.

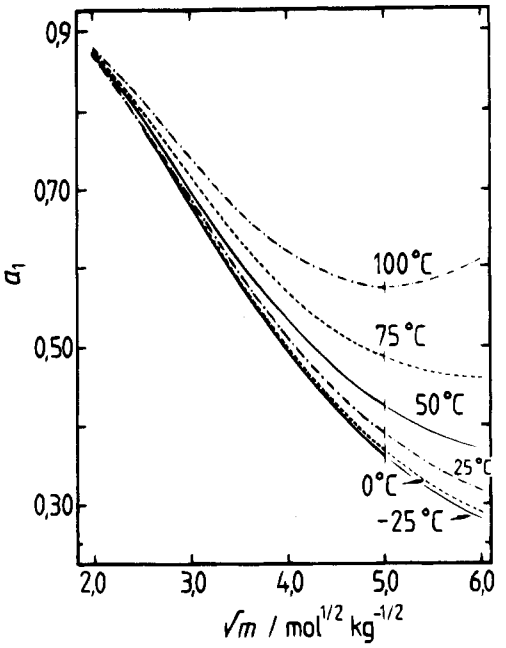

Figure 17. Calculated water activities of pure aqueous $(NH_4)_2SO_4$ from −25 to +100 °C, to high supersaturation. Note that values for $m^{1/2}$ > 5 mol$^{1/2}$ kg$^{-1/2}$ at all temperatures are extrapolations beyond the fitted EDB data.

7. Discussion

The results presented here enable osmotic and activity coefficients, and saturation with respect to solid phases ice and $(NH_4)_2SO_{4(cr)}$, to be calculated for pure aqueous $(NH_4)_2SO_4$ from <273 to 373 K and subsaturated molalities. Properties of supersaturated solutions have also been measured, and are represented by the fitted model to about 25 mol kg^{-1}, though with small deviations from the measured water activities. Comparisons with other data in Figure 15 show that extrapolation to even higher molalities still gives reasonable predictions at 298.15 K. The cause of the differences between the three sets of data shown in Figure 15 is unclear, though it is presumably related to variations in experimental technique and apparatus. Certainly, in the present experiments, the derivation of thermal properties and agreement with other thermal data suggest that the results are self-consistent.

The model is least well constrained at high temperatures and high concentrations. Boiling point elevations, used to derive partial molar heat capacities and model parameters P^J (eq 10), extend only to about 8 mol kg^{-1}. Model calculations of activity coefficients at higher molalities (and $T \neq$ 298.15 K) effectively include an extrapolation of partial molar heat capacities and their influence on activities. The effect of this is illustrated in Figure 17 which shows calculated water activities over a wide range of molality and temperature. It is clear that values for molalities above 25 mol kg^{-1} and temperatures above 323.15 K are unrealistic, showing *increases* in a_1 with molality. Consequently, the limited amount of heat capacity information used to parameterize the model should be borne in mind when estimating the properties of supersaturated solutions at temperatures other than 298.15 K: predictions are likely to become increasingly inaccurate where molalities are greater than 8–10 mol kg^{-1} *and* temperatures are outside of the range 273.15 to about 323.15 K.

The parameters presented in Table 3 for the mole-fraction-based thermodynamic model will, in the future, enable the properties of mixtures containing the ions NH_4^+ and SO_4^{2-} to be calculated as functions of temperature.

Acknowledgment

The authors are grateful to Dr. Barbara Wyslouzil for allowing us access to unpublished data, and to Dr. Ignatius Tang for supplying us with some of his original measurements for aqueous ammonium sulfate and other solutions.

Literature Cited

(1) Clarke, A. D.; Ahlquist, N. C.; Covert, D. S. *J. Geophys. Res.* **1987**, *92*, 4179–4190.
(2) Seinfeld, J. H. *Atmospheric Chemistry and Physics of Air Pollution*; John Wiley and Sons: New York, 1986.
(3) Spann, J. F.; Richardson, C. B. *Atmos. Environ.* **1985**, *19*, 819–825.
(4) Tang, I. N.; Munkelwitz, H. R.; Wang, N. *J. Colloid Interface Sci.* **1986**, *114*, 409–416.
(5) Clegg, S. L.; Pitzer, K. S.; Brimblecombe, P. *J. Phys. Chem.* **1992**, *96*, 9470–9479; **1994**, *98*, 1368; **1995**, *99*, 6755.
(6) Clegg, S. L.; Brimblecombe, P. *J. Chem. Eng. Data* **1995**, *40*, 43–64.
(7) Clegg, S. L.; Brimblecombe, P. *J. Aerosol Sci.* **1995**, *26*, 19–38.
(8) Robinson, R. A.; Stokes, R. H. *Electrolyte Solutions*, 2nd ed. (revised); Butterworths: London, 1965.
(9) Harned, H. S.; Owen, B. B. *The Physical Chemistry of Electrolytic Solutions*; Reinhold: New York, 1958.
(10) Davis, E. J. In *Advances in Chemical Engineering*; Wei, J., Ed.; Academic Press: New York, 1992; Vol. 18, pp 1–94.
(11) Tang, I. N.; Munkelwitz, H. R. *J. Geophys. Res.* **1994**, *99*, 18801–18808.
(12) Bar-Ziv, E.; Sarofim, A. F. *Prog. Energy Combust. Sci.* **1991**, *17*, 1–65.
(13) Chan, C. K.; Flagan, R. C.; Seinfeld, J. H. *Atmos. Environ.* **1992**, *26A*, 1661–1673.
(14) Cohen, M. D.; Flagan, R. C.; Seinfeld, J. H. *J. Phys. Chem.* **1987**, *91*, 4563–4574.
(15) Wyslouzil, B. Unpublished data.
(16) Wishaw, B. F.; Stokes, R. H. *Trans. Faraday Soc.* **1954**, *50*, 952–954.
(17) Filippov, V. K.; Charykova, M. V.; Trofimov, Yu. M. *J. Appl. Chem. USSR* **1986**, *58*, 1807–1811.
(18) Klotz, I. M.; Rosenberg, R. M. *Chemical Thermodynamics, Basic Theory and Methods*, 3rd ed.; Benjamin/Cummings: Menlo Park, CA, 1972.
(19) Young, T. F. *Chem. Rev.* **1933**, *13*, 103–110.
(20) Carslaw, K. S.; Clegg, S. L.; Brimblecombe, P. *J. Phys. Chem.* **1995**, *99*, 11557–11574.
(21) Scatchard, G.; Prentiss, S. S. *J. Am. Chem. Soc.* **1932**, *54*, 2696–2705.
(22) Verrall, R. E. *J. Solution Chem.* **1975**, *4*, 319–329.
(23) Rard, J. A.; Platford, R. F. In *Activity Coefficients in Electrolyte Solutions*, 2nd ed.; Pitzer, K. S., Ed.; CRC Press: Boca Raton, FL, 1991; pp 209–277.
(24) Hill, P. G. *J. Phys. Chem. Ref. Data* **1990**, *19*, 1223–1274.
(25) Johnston, S. M. *Trans.–R. Soc. Edinburgh* **1906**, *45*, 193–240.
(26) Emons, H. H.; Hahn, W. *Wiss. Z. Tech. Hochsch. Chem. "Carl Schorlemmer" Leuna-Merseburg* **1970**, *12*, 129–132.
(27) Chatterji, A. C.; Rastogi, R. P. *J. Indian Chem. Soc.* **1954**, *31*, 63–68.
(28) Timmermans, J. *The Physico-chemical Constants of Binary Systems in Concentrated Solutions*; Interscience: New York, 1960; Vol. 4.
(29) Tang, I. N.; Munkelwitz, H. R. *Atmos. Environ.* **1993**, *27A*, 467–473.
(30) Sukhatme, S. P.; Saikhedkar, N. *Indian J. Technol.* **1969**, *7*, 1–4.
(31) Schneider, W.; Muller, H.; Morke, C. *Chem. Tech. (Leipzig)* **1982**, *34*, 31–32.
(32) D'ans, J.; Surawski, H.; Synowietz. In *Landolt-Börnstein Tables*; Schäfer, Kl., Ed.; Springer-Verlag: Berlin, 1977; New Series, Group IV, Vol. 1, Part b, p 276.
(33) Wagman, D. D.; Evans, W. H.; Parker, V. B.; Schumm, I. H.; Bailey, S. M.; Churney, K. L.; Nuttall, R. L. *J. Phys. Chem. Ref. Data* **1982**, *11*, Suppl. No. 2, 392 pp.
(34) Washburn, E. W., Ed. *International Critical Tables of Numerical Data, Physics, Chemistry and Technology*; McGraw-Hill: New York, 1926; Vol. I.
(35) Weast, R. C., Ed. *CRC Handbook of Chemistry and Physics*, 64th ed.; CRC Press: Boca Raton, FL, 1983.
(36) Desnoyers, J. E.; de Visser, C.; Perron, G.; Picker, P. *J. Solution Chem.* **1976**, *5*, 605–616.
(37) Richardson, R. A.; Spann, J. F. *J. Aerosol Sci.* **1984**, *15*, 563–571.
(38) Cohen, M. D. Ph.D. Thesis, California Institute of Technology, Pasadena, CA, 1987.
(39) Pitzer, K. S. In *Activity Coefficients in Electrolyte Solutions*, 2nd ed.; Pitzer, K. S., Ed.; CRC Press: Boca Raton, FL, 1991; pp 75–153.
(40) De Coppet, L. C. *J. Phys. Chem.* **1904**, *8*, 531–538.
(41) Jones, H. C.; Getman, F. H. *Z. Phys. Chem.* **1903**, *46*, 244–286.
(42) Sborgi, U.; Bovalini, E. *Gazz. Chim. Ital.* **1924**, *54*, 919–956.
(43) Emons, H. H.; Kloth, H. *Wiss. Z. Tech. Hochsch. Chem. "Carl Schorlemmer" Leuna-Merseburg* **1968**, *10*, 102–106.
(44) Silcock, H. L. *Solubilities of Inorganic and Organic Compounds*; Pergamon: Oxford, 1979; Vol. 3.
(45) Schiff, H. *Justus Leibigs Ann. Chem.* **1859**, *109*, 325–332.
(46) Benrath, A.; Thiemann, W. *Z. Anorg. Allg. Chem.* **1932**, *208*, 183–193.
(47) Sommer, F.; Weise, K. *Z. Anorg. Allg. Chem.* **1916**, *94*, 51–91.
(48) D'ans, J.; Freund, H. E.; Woelk, N. H. In *Landolt-Börnstein Tables*; Schäfer, Kl., Lax, E., Eds.; Springer-Verlag: Berlin, 1962; 6th Series, Vol. II, Part 2b, p 3–56.
(49) Frolov, Y. G.; Nasonova, G. I. *Russ. J. Phys. Chem.* **1974**, *48*, 367–369.
(50) Apelblat, A. *J. Chem. Thermodyn.* **1993**, *25*, 1513–1520.
(51) Edgar, G.; Swan, W. O. *J. Am. Chem. Soc.* **1922**, *44*, 570–577.
(52) Diesnis, M. *Ann. Chim. (Paris)* **1937**, *7*, 5–69.
(53) Wexler, A.; Hasegawa, S. *J. Res. Natl. Bur. Stand.* **1954**, *53*, 19–26.
(54) Buchanan, J. Y. *Trans.–R. Soc. Edinburgh* **1899**, *29*, 529–573.
(55) Beggerow, G. In *Landolt-Börnstein Tables*; Schäfer, Kl., Ed.; Springer-Verlag: Berlin, 1976; New Series, Group IV, Vol. 2, p 85.
(56) Britton, H. T. S. *J. Chem. Soc.* **1921**, *121*, 2612–2616.
(57) Weston, A. *J. Chem. Soc.* **1921**, *121*, 2223–1237.
(58) Caven, R. M.; Mitchell, T. C. *J. Chem. Soc.* **1924**, *125*, 1428.
(59) Schreinemakers, F. A. H. *Z. Phys. Chem., Stoechiom. Verwandtschaftsl.* **1910**, *71*, 109–116.
(60) Schreinemakers, F. A. H. *Z. Phys. Chem., Stoechiom. Verwandtschaftl.* **1909**, *69*, 557–568.
(61) Tammann, G. *Wiedemann's Ann.* **1885**, *24*, 523–569.
(62) Rossini, F. D.; Wagman, D. D.; Evans, W. H.; Levine, S.; Jaffe, I. NBS Circular 500 - Part I; U.S. Government Printing Office: Washington, DC, 1961.
(63) Rossini, F. D.; Wagman, D. D.; Evans, W. H.; Levine, S.; Jaffe, I. NBS Circular 500 - Part II; U.S. Government Printing Office: Washington, DC, 1961.
(64) Washburn, E. W., Ed. *International Critical Tables of Numerical Data, Physics, Chemistry and Technology*; McGraw-Hill: New York, 1929; Vol. V.

Received for review February 22, 1995. Accepted May 25, 1995.[⊗] This work was carried out under the auspices of the UK/Hong Kong Joint Research Scheme, funded by the British Council and Hong Kong Research Grants Council.

JE9500441

[⊗] Abstract published in *Advance ACS Abstracts,* August 1, 1995.